Effect of Fiber Content on Void Morphology in Resin Transfer Molded E-Glass/Epoxy Composites

Youssef K. Hamidi
Ecole Nationale des Science Appliquées Safi,
Université Cadi Ayyad,
BP 63, 46000 Safi, Morocco

Sudha Dharmavaram

Levent Aktas

M. Cengiz Altan[1]
e-mail: altan@ou.edu

School of Aerospace and Mechanical Engineering,
University of Oklahoma,
Norman, OK 73019

Effect of fiber volume fraction on occurrence, morphology, and spatial distribution of microvoids in resin transfer molded E-glass/epoxy composites is investigated. Three disk-shaped center-gated composite parts containing 8, 12, and 16 layers of randomly-oriented, E-glass fiber perform are molded, yielding 13.5%, 20.5%, and 27.5% fiber volume fractions. Voids are evaluated by microscopic image analysis of the samples obtained along the radius of these disk-shaped composites. The number of voids is found to decrease moderately with increasing fiber content. Void areal density decreased from 10.5 voids/mm^2 to 9.5 voids/mm^2 as fiber content is increased from 13.5% to 27.5%. Similarly, void volume fraction decreased from 3.1% to 2.5%. Increasing fiber volume fraction from 13.5% to 27.5% is found to lower the contribution of irregularly-shaped voids from 40% of total voids down to 22.4%. Along the radial direction, combined effects of void formation by mechanical entrapment and void mobility are shown to yield a spatially complex void distribution. However, increasing fiber content is observed to affect the void formation mechanisms as more voids are able to move toward the exit vents during molding. These findings are believed to be applicable not only to resin transfer molding but generally to liquid composite molding processes.
[DOI: 10.1115/1.3030944]

Keywords: resin transfer molding, void morphology, fiber content, microscopic image analysis

1 Introduction

Resin transfer molding (RTM) and vacuum assisted resin transfer molding (VARTM), among other composites manufacturing processes, have been established as versatile and simple methods of fabricating medium to large, complex composite structures [1–4]. They are inexpensive ways to integrate large number of components into one part, thereby minimizing the number of parts in an application [5]. In the RTM process, a dry fibrous reinforcement preform is placed inside a mold cavity. Later a reacting liquid resin is injected into the mold cavity to impregnate the preform. Before demolding, the composite part is allowed to cure. Major industries such as aerospace, defense, and automotive generally require parts to be of high performance and excellent surface finish. The formation of flow-induced defects such as voids and dry spots often limits a wider usage of RTM in these fields since void presence has been amply documented to degrade the physical and mechanical properties of the molded composite [6–11]. Although some of these defects and, to some extent, voids can be reduced by the help of vacuum, placement of the vacuum ports and sealing the mold would further complicate the process.

Void formation mechanisms in RTM composites received considerable interest [12–16]. Several researchers studied the influence of various process parameters such as injection pressure, injection rate, cure pressure, cure temperature, preform architecture, fiber sizing, and physicochemical properties of the resin on void formation in RTM composites [7,12–18]. Nonetheless, correlations between void content and other basic parameters such as fiber fraction are not yet established.

Identifying void formation mechanisms in RTM composites can help understand the effect of most of these parameters. At the macroscale, preform impregnation in RTM is generally described by a Darcy flow [19,20]. At the microscale, however, the uneven distribution of fibers leads to interesting flow dynamics as two distinct flows develop: a flow between fiber tows (called viscous flow) and another inside fiber bundles driven by capillary forces (also known as capillary flow). Both flows usually advance at unequal front velocities, thus favoring void formation [12–16]. At higher injection rates, the viscous flow leads the impregnation, and air bubbles are generally trapped inside fiber tows by fingering, resulting in microscopic intratow voids. At slower rates, on the other hand, the capillary flow leads the impregnation, and macroscopic intertow voids are trapped between fiber tows. An optimum void occurrence can be obtained when both flows are advancing at comparable front velocities. This microscale flow behavior has been documented in detail experimentally [12–16]. The capillary number, a nondimensional number defined as the ratio of viscous to capillary forces, has been often used to analyze the movement of fluid fronts and thus predict void formation.

Mahale et al. [12] reported minimal void formation when the filling is performed at the capillary number range of 2.5×10^{-3}. Later, Patel and co-workers [13–16] reported the existence of a master curve of void content as a function of the modified capillary number that includes the resin/fiber contact angle in the analysis. Several subsequent theoretical and experimental studies have analyzed void formation data in terms of the modified capillary number [21–26], thus establishing the capillary number analysis as a method for predicting void formation in RTM composites. Other theoretical and numerical models have been pro-

[1]Corresponding author.

Contributed by the Materials Division of ASME for publication in the JOURNAL OF ENGINEERING MATERIALS AND TECHNOLOGY. Manuscript received May 30, 2005; final manuscript received October 13, 2008; published online March 9, 2009. Review conducted by Hussein Zbib. Paper presented at the 2005 ASME International Mechanical Engineering Congress (IMECE2005), Orlando, FL, November 5–11, 2005.

posed for predicting void occurrence in liquid injection processes [27–32]. However, these models often have limited range of application as they are generally developed for simplified preform architectures.

Higher fiber content in RTM composites would lead to faster fluid flow velocities as the empty space for resin flow is reduced. Therefore, void occurrence would change depending on the capillary number range experienced during filling. Higher injection rates are more consistent with most industrial practices, and increasing fiber content in these cases would consequently increase the viscous flow and thus induce a sharp increase in void formation [12–16]. On the other hand, impregnating higher fiber contents would require higher injection pressures [19,20], and higher filling pressures are known to reduce void occurrence [17,25,32]. In addition, voids can only occur within the resin, hence reducing the total volume of the resin would possibly reduce void formation and consequently lead to lower void occurrence. Therefore, the effect of fiber content on void occurrence within RTM composites cannot be predicted using the available analysis tools and thus requires additional investigation.

Very few studies are available in literature regarding the effect of fiber content on voids in composite materials, and most of these studies do not focus on void formation [2,22,33]. Abraham and Mcllhagger [2], for example, visually inspected void content and wet out for RTM composites fabricated under the same conditions and containing 18% and 50% fiber volume fractions. Increasing the fiber content was reported to change the void content from low to high and wet out quality from good to incomplete.

Rajulu et al. [33], on the other hand, studied short bamboo fiber-epoxy composites at fiber contents of 10%, 20%, 30%, and 40% by volume. The authors reported that void content decreased almost linearly with increasing fiber content. Increasing the fiber volume fraction from 10% to 40% induced an 84% reduction in void content from 1.43% to 0.23%. Kang et al. [22] studied void formation in RTM composites molded under similar processing conditions at two fiber contents, i.e., 19.2% and 63.9%. The authors reported comparable void areal densities for the two fiber contents. However, lower void content and smaller voids were reported at the higher fiber content. These conflicting results also do not show any direct effect of increasing fiber content on void occurrence. Consequently, a systematic study on the effect of fiber content on void occurrence and morphology in RTM composites can enhance our understanding of void formation and ultimately help determining optimum RTM parameters for lowering void occurrence. To the best of our knowledge, no such study exists in literature.

In the current study, effects of fiber volume fraction on void content, void morphology, and spatial void distribution are investigated for resin transfer molded E-glass/epoxy composites. Three composite disks are molded under the same process parameters at 13.5%, 20.5%, and 27.5% fiber volume fractions. Voidage in each disk is assessed by microscopic image analysis, and differences in void content and void areal density are evaluated. In addition, changes in void morphology (i.e., size and shape) induced by increasing fiber content are investigated. Furthermore, radial variation in void content and void's proximity to fibers are examined for the three fiber contents studied.

2 Experimental Setup

2.1 Molding Procedure. Three composite disks containing 13.5%, 20.5%, and 27.5% E-glass fibers by volume are fabricated in this study using an experimental RTM apparatus. This custom-made molding setup comprises a hydraulic press, two reservoirs for resin and curing agent, a static mixer, and a disk-shaped mold cavity. When operated, the molding press forces the EPON 815C resin and EPICURE 3282 (Shell Chemicals) curing agent out of the reservoirs into the mold cavity at a constant flow rate. Before molding, both fluids are degassed in an ultrasonic bath at 50 kHz for 15 min since sonicating is reported to reduce void formation due to volatile or entrapped moisture in the resin [4–6,17,34]. These fluids are thoroughly mixed by the static mixer containing 32 alternating helical segments, thus yielding a gel time of approximately 20 min. 8, 12, and 16 layers of the randomly-oriented, chopped-strand, E-glass fiber mats with a planar density of 0.2152 ± 0.0063 kg/m^2 (Fiberglast Part No. 248) are, respectively, placed in the mold cavity prior to filling. The details of the molding procedure and experimental setup are described in detail elsewhere [20,23–26].

2.2 Sample Preparation for Microscopic Image Analysis. The planar isotropy of the fibrous preform and the mold axisymmetry simplify the impregnation into a purely radial flow. Therefore, the molded disks are studied along their radii. Three radial samples, one from each disk, are cut and prepared for microscopic image analysis. All samples are 75 mm long, while their average thicknesses are measured as 4.93 mm, 4.91 mm, and 4.90 mm for composites containing 13.5%, 20.5%, and 27.5% fibers, respectively. Less than 1% variation recorded in the average sample thickness indicates that the deflection of the mold walls was not significant enough to affect the impregnation kinematics of the samples molded at three different fiber volume fractions. Radial variation in voidage is assessed by dividing each 75-mm-long sample into five 15-mm-long regions along the radial direction. Composite strips are embedded separately into a quick cure acrylic resin (Allied High Tech. Products, Part No. 170). For polishing, a series of polishing pastes is applied (Clover Compound) with grit sizes ranging from 180 (i.e., 80 μm average particle diameter) to 1200 (15 μm) in six successive steps. To remove paste residues after each step, 40 min of subsequent cleaning periods are performed in an ultrasonic bath at 50 kHz. Thereafter, the samples are ready for microscopic image analysis.

2.3 Void Characterization. Microscopic image analysis has been reported to be among the most precise techniques for measuring void contents [7,11,35–37]. In addition, this method provides detailed information on other essential parameters such as void location, shape, and size that cannot be assessed by other methods. Frequently, microscopic image analysis is utilized by randomly averaging selected frames of the studied composite sample [35,36]. In contrast, the entire cross sections of the studied composite samples are scanned in the current investigation in order to accurately estimate void content, morphology, and their spatial variations. Voidage features are obtained from images acquired at 200× magnification using a PC-based charge coupled device (CCD) camera mounted on a MEIJI light microscope. At this particular magnification, every frame displays approximately a 0.71×0.53 mm^2 area. Hence, a total of 4320 frames are captured (1440 frames for each fiber fraction). The selected magnification of 200× enables the assessment of voids as small as the radius of a single fiber of 7 μm. Consequently, all identifiable voids throughout the entire composite samples are included in the analysis of void content and morphology. In this study, all voids are identified by hand since automatic thresholding—usually used image analysis of voids—is reported to induce errors in void content measurement due to statistical uncertainty, pixel size, threshold levels used, and the lighting variations in different areas of the same frame [38,39]. Each captured frame is processed using the image analysis software IMAGE TOOL®, which allows the measurement of voids' area, A, and maximum length, L_{max}. Thereafter, all voids are visually identified. A total of 9484 voids are identified in all three samples; specifically 3364, 3095, and 3025 voids are identified for the composites containing 13.5%, 20.5%, and 27.5% fibers, respectively. Each void boundary is traced by hand to capture its morphological features. A statistical error analysis of voidage measurement is performed on a group of 100 voids of various shapes and sizes. Each void's area and maximum length are measured five times. The variation originating from this manual tracing method is shown to be less than 1% in all measurements. In addition, the results are not affected by the skills and judgment of

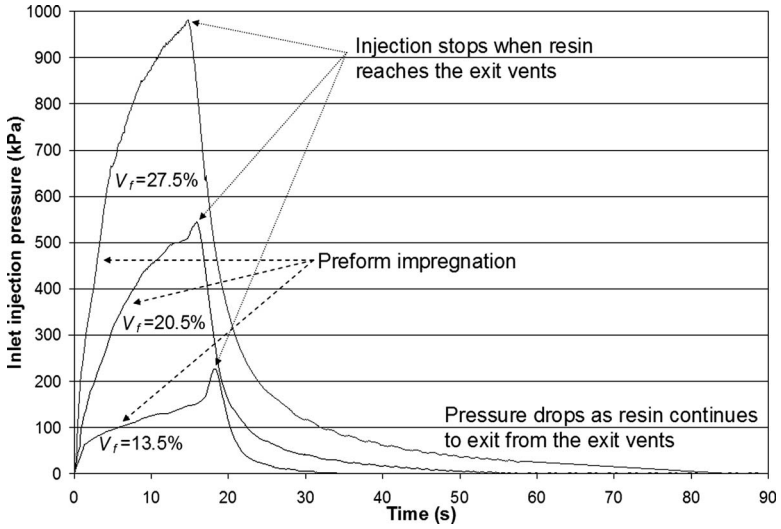

Fig. 1 Effect of fiber content on the inlet pressure profiles during molding

the operator performing the tracing as two different operators independently obtained identical void content results on the selected test samples.

3 Results and Discussion

3.1 Inlet Mold Filling Pressure. Inlet pressure variation during molding is monitored with a flush diaphragm pressure transducer (Sensotec® BP357BR Model S, 0.1% accuracy), inserted between the static mixer and the mold inlet. As a result of the circular mold geometry and the preform planar isotropy, the resin front has a circular shape and advances radially through the preform. Since molding is performed at a constant flow rate, the resin front moves at higher velocities closer to the injection gate. At constant flow rate, the inlet pressure increases as the flow front advances so that the larger preform area can be impregnated. Inlet pressure data recorded during filling of all three disks are shown in Fig. 1.

During the first 15 s of mold filling, the inlet pressures increase at different rates for the three composites. The maximum inlet pressure recorded for each composite significantly increases with increasing fiber content. A maximum inlet pressure of 980 kPa is attained at the end of filling for the composite containing 27.5% fibers by volume, while maximum inlet pressures of 515 kPa and 165 kPa are recorded when molding the 20.5% and 13.5% fiber content composites, respectively. This large difference in injection pressure (almost two- and sixfold) can affect void formation and mobility during filling. Higher injection pressures might shrink the air bubbles entrapped by the advancing fluid front and thus yield lower void content at higher fiber volume fractions. At the end of filling, pressure readings of the composites molded at 13.5% and 20.5% fiber contents show slight increases needed to force the resin into the constricted channel spacing between mold walls and spacer plates. Once the resin reaches the exit vents, the molding press is turned off, stopping resin injection. As seen in Fig. 1, for all three fiber contents, a monotonic decrease down to zero gauge pressure is recorded after the injection is stopped.

3.2 Effect of Fiber Content on Void Occurrence. Representative images obtained at 200× magnification from the 13.5%, 20.5%, and 27.5% fiber content composites are depicted in Fig. 2. Figure 2 also shows the difference in fiber concentration observed between the three composite samples. Fibers are seen as more homogeneously distributed through the composite molded with 27.5% fibers by volume, while the composite molded with 13.5% fiber content contains large matrix-rich regions and other zones with high fiber concentration.

Void contents and void areal densities of the molded composites are shown in Fig. 3. Both void content and void areal density are observed to decrease with increasing fiber content. Void areal density is observed to decrease from 10.5 voids/mm^2 in the composite molded with 13.5% fiber content to 9.7 voids/mm^2 and 9.5 voids/mm^2 at 20.5% and 27.5% fiber contents, respectively. A similar trend is observed for void content. A void content of 3.1% is measured for the composite containing 13.5% fibers by volume. Slightly smaller void contents of 2.7% and 2.5% are measured, respectively, at 20.5% and 27.5% fiber contents. The respective 12.9% and 18.3% reduction rates in void content corroborate the results obtained by Kang et al. [22] and can be attributed to lower matrix volume, more uniform preform architecture, and higher injection pressure at higher fiber content.

3.3 Effect of Fiber Content on Void Location. Void proximity to fibers can help understand their formation mechanisms [23–26] as well as their effects on mechanical performance of the composite part. Three different void locations are defined within the molded composites. The first location is defined as areas rich in matrix. Voids in this location are entirely enveloped by the

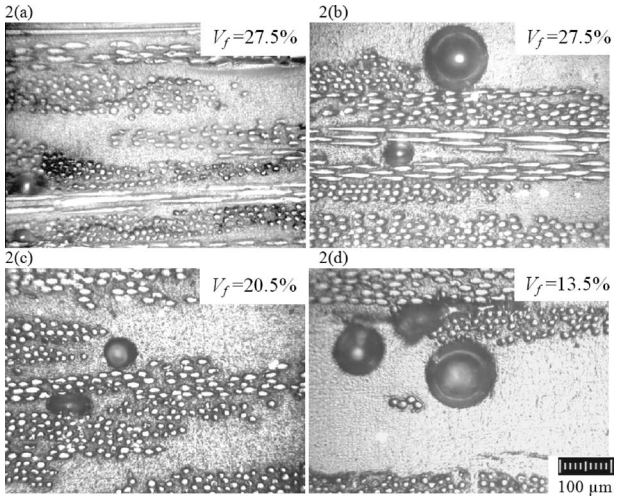

Fig. 2 Representative images of the composites molded with different fiber volume fractions, V_f, obtained at 200× magnification

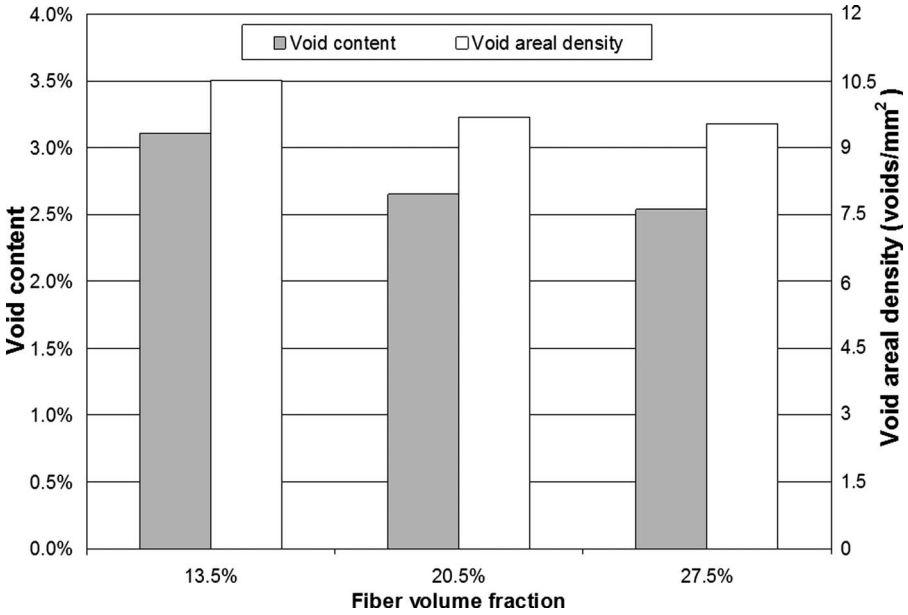

Fig. 3 Effect of fiber content on void content and void areal density

epoxy matrix and are called matrix voids. The second location is defined as areas rich in preform, where the area is primarily composed of reinforcing fibers. Voids in this region are intratow voids and are referred to as preform voids. Finally, the remaining voids positioned next to, but not within the fiber bundles are called transition voids. According to this classification, voids trapped between fiber bundles in Fig. 2(*a*) and at the bottom of Fig. 2(*c*) are considered preform voids. Voids seen in the top of Fig. 2(*b*) and at the center of Fig. 2(*d*) represent transition voids, and the void located at the left of Fig. 2(*d*) is an example of matrix voids.

Figures 4(*a*) and 4(*b*) show respective contributions to void content and void areal density from voids in different locations within the composites. At all three fiber contents, matrix voids have the lowest contribution to void content and void areal density. In addition, both void content and void areal density of matrix voids decrease steadily with increasing fiber content. Matrix void content decreases from 0.4% at V_f=13.5% to 0.3% at V_f =20.5%, then reaches 0.2% at V_f=27.5%. Simultaneously, matrix void's areal density is observed to decrease from 1.4 to 1.0 and 0.7 voids/mm^2.

Preform void content shows a somewhat similar trend. Contribution of preform voids to void content slightly decreases from 1.1% measured in both composites molded at V_f=13.5% and 20.5% to 1.0% at V_f=27.5% (Fig. 4(*a*)). Preform void's areal density (Fig. 4(*b*)), on the other hand, is observed to increase from 4.6 at V_f=13.5% to 5.4 and 5.3 voids/mm^2 at V_f=20.5% and 27.5%, respectively. The small reduction in void content and almost 17% increase in void areal density suggest that preform voids become smaller at higher fiber contents. Transition voids, on the other hand, do not show any clear trend.

However, combined contributions from voids located within or right next to fiber bundles to either void content or void areal density are observed to increase, in percentage, with increasing fiber content. The percentage of void content originating from preform and transition voids rises from 88.9% at V_f=13.5% to 89.4% at V_f=20.5% and reaches 92.5% at V_f=27.5%. The similarly defined percentage for void areal density also increases from 86.9% at V_f=13.5% to 89.5% at V_f=20.5% and reaches 92.8% at V_f=27.5%. The high occurrence of voids within and next to the preform is consistent with the range of modified capillary number experienced during these molding experiments (later calculated to change from 0.12 to 1.65, see Table 1). These relatively high values of capillary number predict that most formed voids would be entrapped either inside or adjacent to fiber bundles [12–16,23–26].

3.4 Effect of Fiber Content on Void Size. In order to classify void sizes, an equivalent diameter, D_{eq}, is defined for each void as

$$D_{eq} = \sqrt{\frac{4A}{\pi}} \tag{1}$$

where A is the void area measured via image analysis software UTHSCSA IMAGE TOOL®.

Figure 5 illustrates void size distributions based on D_{eq} for the molded composites. The size distribution of voids shows distinct differences among the three fiber contents. A small shift in void size distribution is observed as the fiber content is increased. The average void size augments from 53 μm at V_f=13.5% to 54 μm and 55 μm at V_f=20.5% and 27.5%, respectively. However, the highest relative contribution to void areal density changes from 20% for voids with 20 μm$<D_{eq}\leq$30 μm at V_f=13.5–23% relative contribution for voids with 30 μm$<D_{eq}\leq$40 μm at V_f =27.5%.

In order to analyze other aspects of void size distributions, three different size categories are introduced. Large voids are defined as those with an equivalent diameter greater than 100 μm, i.e., $D_{eq}>100$ μm, while voids with an equivalent diameter lower than 50 μm are regarded as small voids. Intermediate equivalent diameter values, i.e., 50 μm$<D_{eq}\leq$100 μm, correspond to medium size voids. Figures 6(*a*) and 6(*b*) depict size distributions of void content and void areal density of voids encountered in the molded composites.

As Fig. 6(*b*) indicates, the areal density of small voids is observed to decrease linearly from 5.8 voids/mm^2 to 4.8 voids/mm^2 when the fiber content is increased from 13.5% to 27.5%. However, small voids show almost the same percent contribution of 0.5% to void content for all composites. Large voids see their contribution to both void content (Fig. 6(*a*)) and void areal density (Fig. 6(*b*)) decrease with increasing fiber content, whereas medium voids see some increases in both void content and void areal density. Void content of medium increases in both void content and void areal density. Void content of medium voids augments from 1.6% to 1.8% as fiber content is increased. Simi-

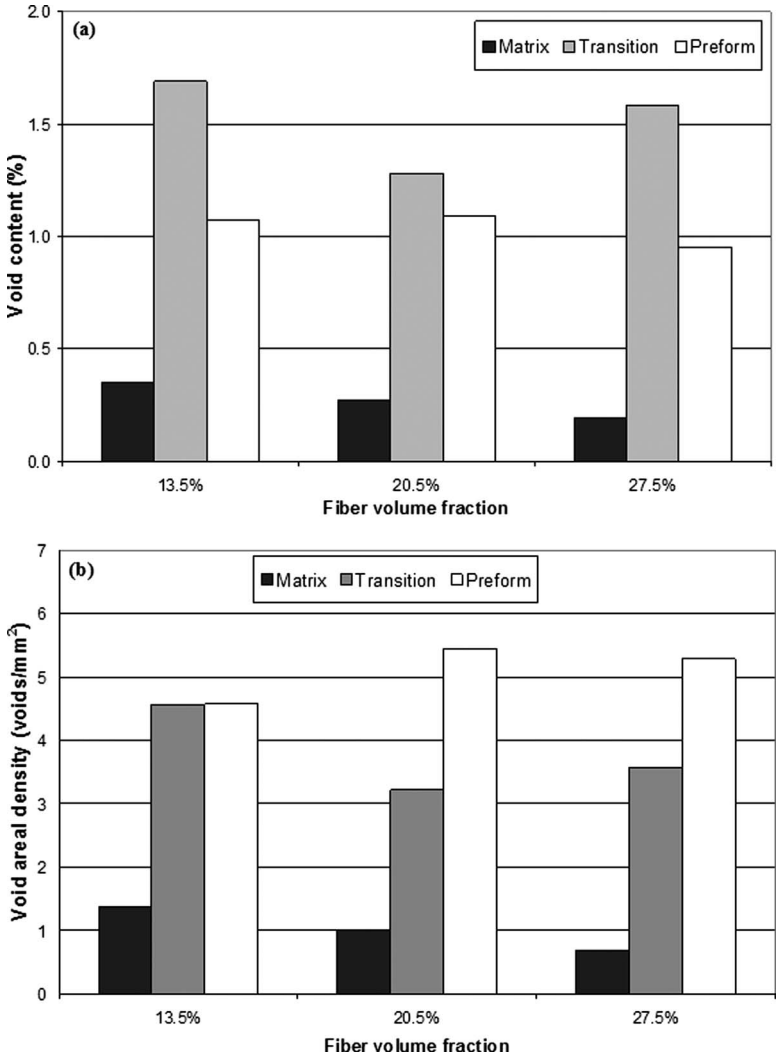

Fig. 4 Effect of fiber content on (*a*) the contributions to void content and (*b*) void areal densities of voids encountered in different composite locations

larly, medium void areal density increases from 3.9 voids/mm^2 to 4.3 voids/mm^2. Therefore, the small increase in average void size observed in Fig. 5 can be solely attributed to the increase in medium voids.

3.5 Effect of Fiber Content on Void Shape. Detrimental effect of voids on mechanical performance of composites is well established. Judd and Wright [6], for example, reported that a void content as low as 1% results in a decrease in strength up to 30% in bending, 3% in tension, 9% in torsional shear, and 8% in impact. Due to variations in void sizes and locations, a variety of void shapes are encountered in RTM composites [7,11–13,22–26,40,41]. Patel et al. [14], for instance, investigated effects of fiber architecture on void formation in liquid composite molded (LCM) composites. Although no quantitative results were given, the authors reported the formation of voids with different shapes for both bidirectional stitched fiberglass and four-harness woven fiberglass preforms.

In more recent studies of voidage effects on mechanical properties, Paton and co-workers [40,41] studied RTM woven carbon/epoxy composites at 59% fiber content and observed two major void shapes. The first consists of spherical to elliptical voids with a diameter of 100–200 μm, and the second represents larger irregularly-shaped voids confined to the preform. The authors reported a 7% reduction in interlaminar shear strength per 1% in-

Table 1 Modified capillary number variation along the radial flow direction for different fiber volume fractions, V_f

Radial distance from the injection gate (mm)		7.5	22.5	37.5	52.5	67.5
V_f=13.5%	Modified capillary number, Ca^*	1.38	0.36	0.22	0.16	0.12
V_f=20.5%		1.50	0.40	0.24	0.17	0.13
V_f=27.5%	$Ca^* = \frac{\mu V}{\gamma \cos \theta}$	1.65	0.43	0.26	0.19	0.14

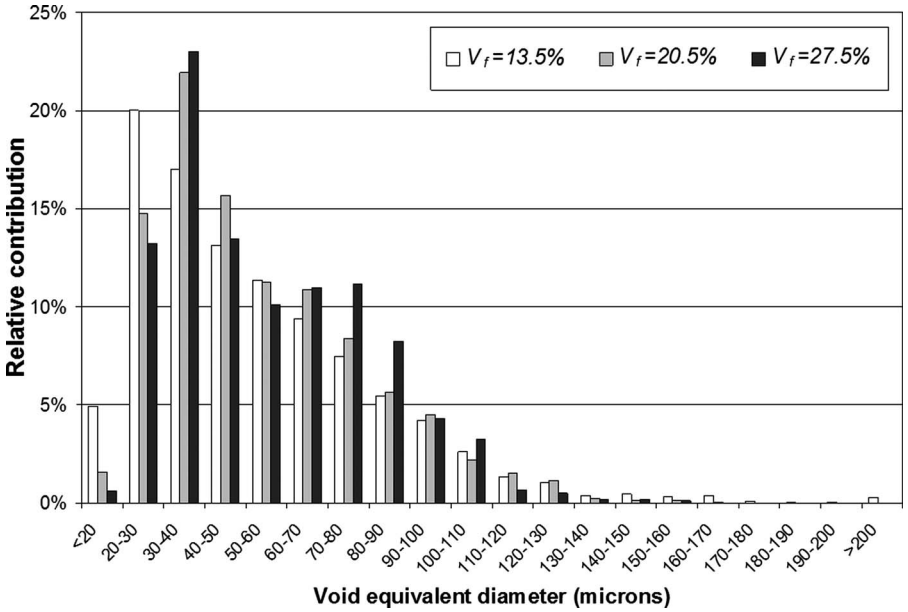

Fig. 5 Effect of fiber content on void size distribution

crease in voidage up to 10% for resin transfer molded composites containing five-harness satin preform. In addition, the authors observed that only irregularly-shaped voids induced early crack formation under loading.

Figure 2 shows images obtained at 200× magnification that depict different void shapes encountered in the three molded composites. Voids seen in the top of Fig. 2(*b*) and at the center of Fig. 2(*d*) are mostly circular. In contrast, voids trapped between fiber bundles in Figs. 2(*a*)–2(*c*) are more elliptical. The voids entrapped within the preform in the top of Fig. 2(*d*) present a different irregular geometry. Based on these observed shapes, voids are separated into two groups: irregular and spherical voids. Irregular voids are defined as those presenting a nonconvex planar surface area, that is, two different points exist within the void that can be connected by a straight line that intersects the void boundary. The remaining voids are mostly spherical, even though most of them do not present a perfect circular symmetry. To classify this variation in voids' roundness, void data are further processed by introducing the shape ratio, R_s, defined for each void as the equivalent diameter obtained from Eq. (1) divided by the maximum measured length, $L_{\max}$, within a void:

$$R_s = \frac{D_{\text{eq}}}{L_{\max}} \tag{2}$$

Note that ideal circles are represented by $R_s = 1$, and as the shape ratio gets smaller, voids become more elongated. Using this shape ratio, spherical voids are further segregated into two categories: circular voids with shape ratios above 0.95 ($0.95 < R_s \leq 1$) and elliptical voids with shape ratios lower than 0.95.

Using the criteria defined above, contributions to void content from voids with different shapes are calculated. The resulting shape distributions of voids observed in the composites molded with different fiber contents are presented in Fig. 7. Shape distributions based on contributions to void content (Fig. 7(*a*)) and relative percentage of void areal density (Fig. 7(*b*)) are simultaneously analyzed in order to assess void morphology in the three composites.

As illustrated in Fig. 7(*a*), circular voids see their contribution to the void content slightly increase from 42.7% to 50.0% as fiber content is increased. Simultaneously, circular void relative percentage augments from 27.7% to 31.7%. Elliptical voids also see their contribution to void content increase from 17.7% to 27.2% as fiber content is increased. Over the same range, circular void relative percentage expands from 22.7% to 25.1% (Fig. 7(*b*)).

Irregular voids, on the other hand, show an opposite trend. Contribution of irregular voids to void content decreases from 39.6% to 22.4%. A slightly smaller decrease is observed in irregular void's contribution to void areal density, as shown in Fig. 7(*b*). These results suggest that as the fiber content is increased, less irregular voids tend to form within the molded composite.

Since large voids with irregular shapes can affect the performance of molded composites more adversely than other void shapes [9,40,41], effect of fiber content on size distribution of irregular voids is investigated. Thus, size distributions of irregular voids based on areal void density are presented in Fig. 8. As Fig. 8 shows, areal densities of irregular voids of all sizes are observed to decrease with increasing fiber content. However, small irregular voids are observed to decrease at a smaller rate. Small void areal density decreases from 3.3 voids/mm^2 to 3.1 voids/mm^2 as fiber content is increased. Large irregular void's occurrence is very limited in all cases and decreases as well from 0.3 voids/mm^2 to 0.05 voids/mm^2 as fiber content is increased. Medium irregular voids see the largest reduction from 1.6 voids/mm^2 to 0.7 voids/mm^2. These results show that irregular voids occur at a lower rate and become primarily small at higher fiber content (e.g., 81.2% of irregular voids are small at V_f=27.5%). Therefore, critical adverse effects of irregular voids have a higher probability at lower fiber contents as only larger irregular voids are reported to induce early crack formation [9,40,41].

3.6 Effect of Fiber Content on Radial Voidage Variation. The modified capillary number, Ca^*, described in the Introduction as the nondimensional ratio of viscous forces to capillary forces is defined as

$$Ca^* = \frac{\mu \cdot V}{\gamma \cos \theta} \tag{3}$$

where μ, V, γ, and θ are the impregnating resin viscosity, the macroscopic fluid front velocity, the resin surface tension, and the liquid-fiber contact angle, respectively. When the modified capillary number changes spatially, one might expect to see not only spatial variations in void content but also variations in void sizes

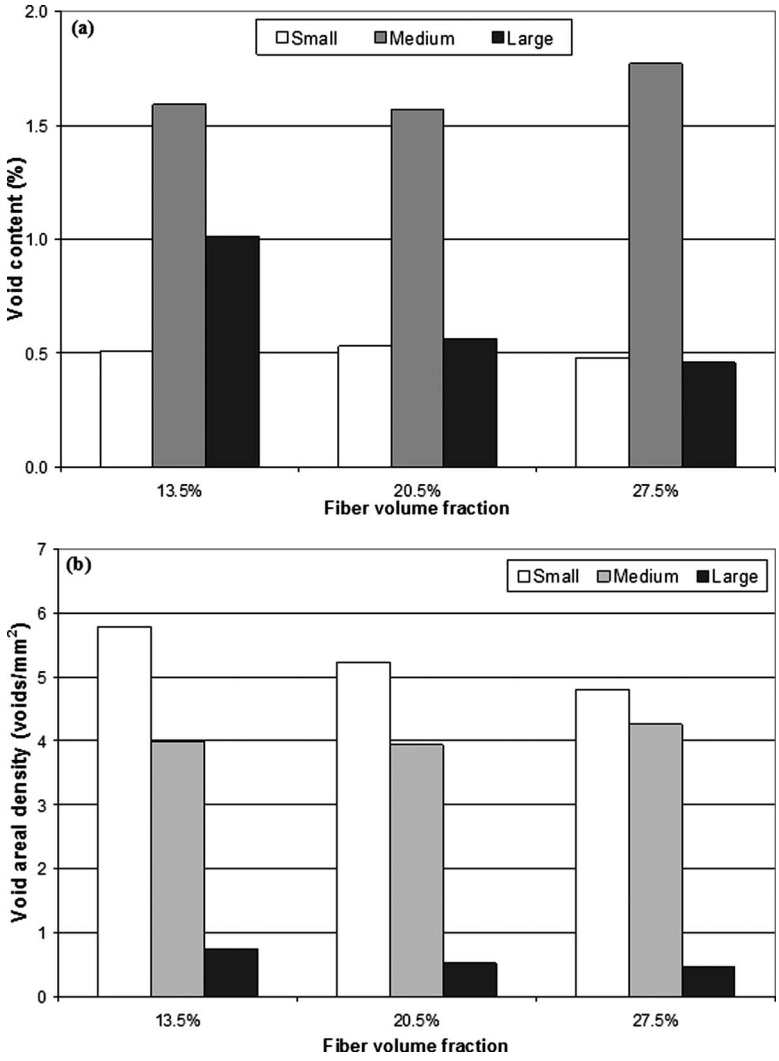

Fig. 6 Effect of fiber content on size distributions based on (*a*) void content and (*b*) void areal density

and shapes. Therefore, evaluating the range of capillary number involved during these RTM experiments can be vital in understanding relevant void formation mechanisms and consequently spatial void distribution and void morphology.

Determining the modified capillary number requires, as described in Eq. (3), quantifying the resin viscosity, μ, the macroscopic fluid front velocity, V_{ave}, the resin surface tension, γ, and the advancing contact angle, θ. Both the surface tension and the advancing contact angle are measured in an earlier study for the same system of resin, curing agent, and E-glass fibers [23–25]. The measured values of the surface tension and advancing contact angle are 36.3×10^{-3} N/m and 34 deg. The viscosity of the resin-curing agent mixture is measured using a Brookfield viscometer (Model DV-II +). Even though the mixture's viscosity changes toward the end of the 20 min gel time, its value remains reasonably stable around 0.96 N s/m^2 during the first few minutes of mixing. The macroscopic fluid front velocity can be determined from the injection flow rate and the mold geometry as

$$V_{\text{ave}} = \frac{Q}{A} = \frac{Q}{2 \cdot \pi \cdot H \cdot r \cdot (1 - V_f)} \tag{4}$$

where Q is the resin flow rate, H is the thickness of the mold, r is the radius at which the capillary number is calculated, A is the cross-sectional area of the resin flow at r, and V_f is the fiber volume fraction. It is clear from Eq. (4) that an increase in fiber volume fraction increases the impregnation velocity, thus affecting the dynamics of void formation. Substituting Eq. (4) in Eq. (3), the modified capillary number becomes a function of the radial distance from the injection gate:

$$Ca^* = \frac{\mu \cdot Q}{2 \cdot \gamma \cdot \pi \cdot H \cdot (1 - V_f)\cos\,\theta} \cdot \frac{1}{r} \tag{5}$$

As described in Sec. 2, each composite sample is divided into five 15-mm-long radial regions; thus the fluid front velocity is evaluated at the center of each radial region. The modified capillary number is obtained by substituting the measured values in Eq. (5). The calculated Ca^* for the different radial distances from the injection gate are presented in Table 1. It should be noted that performing these molding experiments at a constant volume flow rate is desirable since it enables one to accurately determine the fluid front velocity (i.e., effective velocity of the impregnation front). As the modified capillary number during filling is determined for different fiber volume fraction, a meaningful comparison of the void content and morphology can be done among these samples as described below.

As illustrated in Table 1, the Ca^* variation within each composite is far greater than the respective difference in modified capillary numbers from one fiber content to the other. The range of Ca^* measured for all three fiber contents is much larger than the reported Ca^* critical value of 2.5×10^{-3}, where void occurrence is

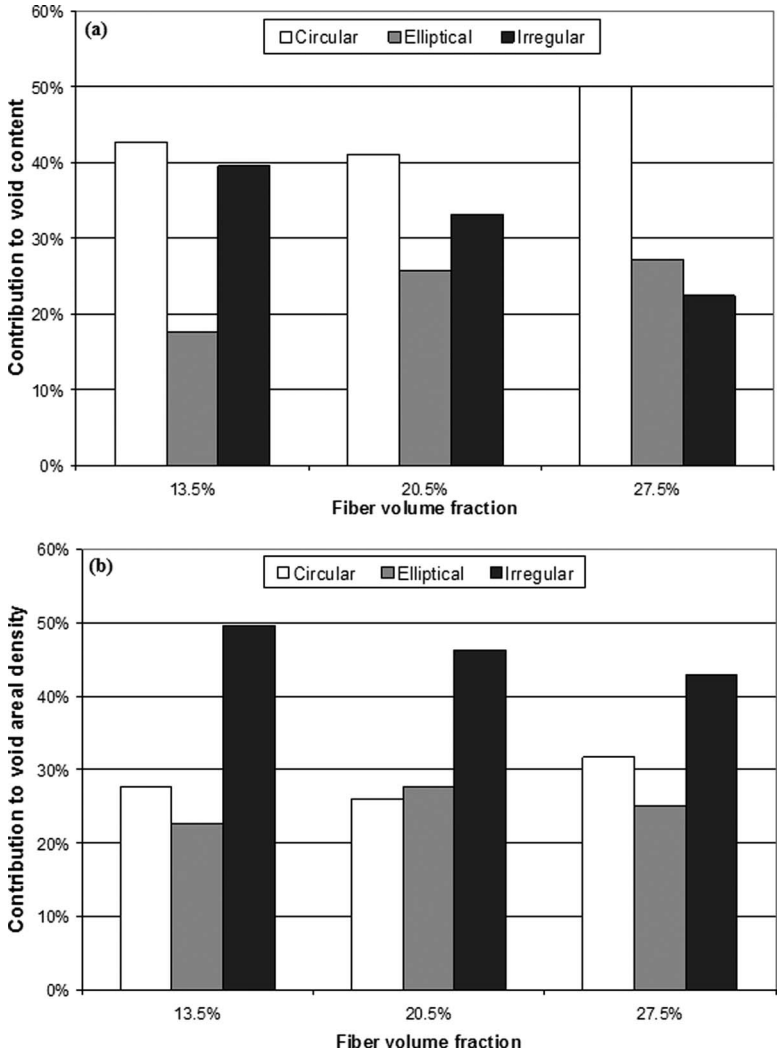

Fig. 7 Effect of fiber content on voidage shape distribution based on (*a*) contribution to void content and (*b*) contribution to void areal density

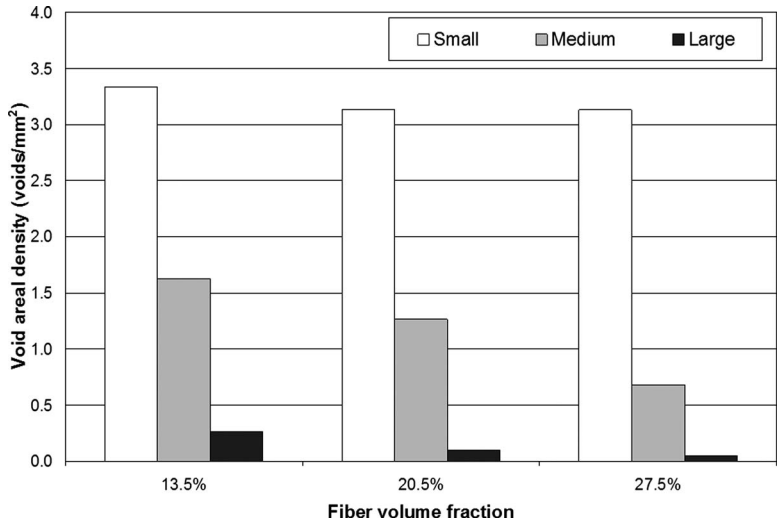

Fig. 8 Effect of fiber content on the size distribution of irregular voids based on areal void density

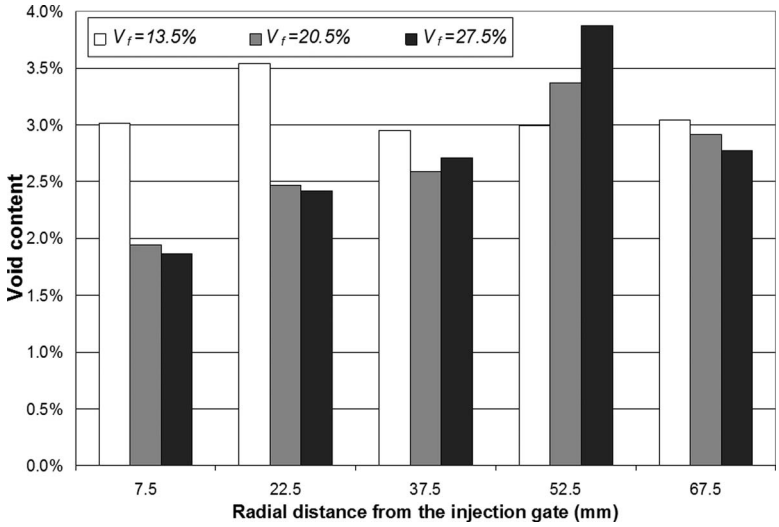

Fig. 9 Effect of fiber content on radial variation in void content

minimal [12–16]. Furthermore, at this high value of Ca^*, formed voids are expected to be dominantly intravoids, that is, located within or right next to fiber tows [12–16,23–26].

Radial variation in void content for the molded composites is presented in Fig. 9. Although void content of the V_f=13.5% composite does not show any clear trend, the other two composites show a net increase in void content with increasing radial distance from the injection gate. Thus, void content is observed to increase from almost 2.0% to well above 2.8% for both composites molded at V_f=20.5% and 27.5%. For both these composites, increases in void content seem to be almost linear between the first and fourth radial regions, reaching 3.4% and 3.9%, respectively.

These increases in void content do not fit the expected trend predicted by the capillary number analysis. As the radial distance from the injection gate increases, the advancing fluid front has to impregnate larger areas and thus becomes slower. Hence and according to the range of modified capillary numbers involved, the resulting void content is expected to decrease away from the inlet. However, Fig. 9 shows an opposite trend at higher fiber contents. As fiber content increases, the maximum pressure during filling rises dramatically. This pressure increase is believed to shrink the trapped voids, considerably facilitating their transport by the flow toward the exit vents. This phenomenon has been already observed in similar RTM composite disks where Ca^* varied during impregnation [23].

This phenomenon can help explain the radial variation in void content for the V_f=13.5% composite. At this fiber content, the moderate pressure experienced during injection is believed to limit void transport, and the result is a somewhat homogeneous radial void content. Thus, as the fiber content is increased, void distribution in RTM composites is more affected by transport dynamics than formation mechanisms.

In order to verify the occurrence of such phenomenon, further analysis is carried out. Voids are further classified into *mobile voids*, i.e., combined matrix and transition voids that can be transported, and *immobile voids* trapped inside fiber tows, i.e., preform voids. Figure 2 shows different mobile and immobile voids. According to this classification, the large circular void seen in the top of Fig. 2(*b*) and the two circular voids in the middle of Fig. 2(*d*) are examples of mobile voids, while the smaller circular void of Fig. 2(*b*) trapped inside the fiber tows and the elliptical void in Fig. 2(*c*) fall into the immobile void category.

The radial variations in mobile and immobile voids are assessed and their ratio is presented in Fig. 10. The ratio of immobile void

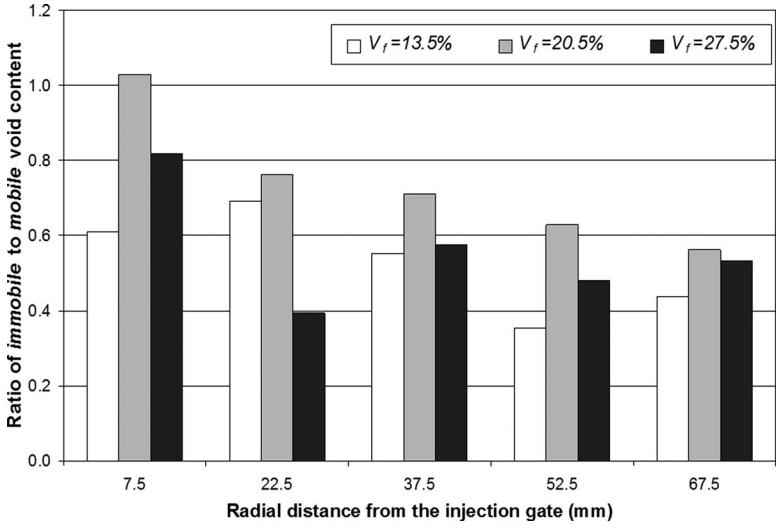

Fig. 10 Effect of fiber content on the radial variation in the ratio of immobile to mobile void content

content to mobile void content can be used to analyze the variation in both void categories along the radius of each composite. In all three composites, this ratio shows a decreasing trend in the radial direction. The immobile to mobile ratio is observed to decrease from 60.9% in the first to 43.7% in the fifth radial region of the V_f=13.5% composite. An even higher reduction is observed at V_f=20.5%. The immobile to mobile ratio is observed to decrease from 103.0% in the first radial region to 56.2% in the fifth. A similar decrease is observed in the composite molded at V_f =27.5%, where the immobile to mobile ratio is observed to decrease from 81.8% in the first radial region to 53.3% in the fifth. Hence, more mobile voids are encountered far from the injection gate for all three fiber contents studied. The ratio of immobile to mobile voids might also be affected by the level of injection pressure. For lower pressures, the number of mobile matrix voids is usually higher, thus leading to a smaller immobile to mobile void ratio throughout the composite. These results confirm the increasing dominance of mobile voids toward the exit vents and furthermore explain the increase in voids at a larger radial distance from the injection gate.

4 Conclusions

The effect of fiber volume fraction on occurrence, morphology, and spatial distribution of voids in resin transfer molded E-glass/epoxy composites was investigated. Three center-gated composite disks were molded at 13.5%, 20.5%, and 27.5% fiber volume fractions. Voids throughout these disk-shaped composites were evaluated via microscopic image analysis of radial samples. All identifiable voids at 200× magnification were assessed and their equivalent radius, area, and shape were measured. Void occurrence is found to decrease moderately with increasing fiber content. Void areal density decreased from 10.5 voids/mm^2 to 9.5 voids/mm^2 as fiber content is increased. Average void size is observed to remain similar at 53–55 μm when the fiber content is increased from 13.5% to 27.5%. Increasing fiber volume fraction from 13.5% to 27.5% is found to lower the contribution of irregularly-shaped voids from 40% of total voids down to 22.4%. Along the radial direction, combined effects of void formation by mechanical entrapment and void mobility are shown to yield a spatially complex void distribution. Increasing fiber content is observed to affect the void formation mechanisms as more voids are able to move toward the exit vents during molding. Thus, both transport dynamics and void formation mechanisms affect spatial conformation of voids. These findings are believed to be applicable not only to resin transfer molding but generally to liquid composite molding processes.

References

[1] Brouwer, W. D., Van Herpt, E. C. F. C., and Labordus, M., 2003, "Vacuum Injection Moulding for Large Structural Applications," Composites, Part A, **34**, pp. 551–558.

[2] Abraham, D., and Mcllhagger, R., 1998, "Investigation Into Various Methods of Liquid Injection to Achieve Mouldings With Minimum Void Content and Full Wet Out," Composites, Part A, **29**, pp. 533–539.

[3] Abraham, D., Matthews, S., and Mcllhagger, R., 1998, "A Comparison of Physical Properties of Glass Fiber Epoxy Composites Produced by Wet Lay-Up With Autoclave Consolidation and Resin Transfer Moulding," Composites, Part A, **29**, pp. 795–801.

[4] Johnson, C. F., 1990, *Composite Materials Technology: Process and Properties*, Hanser, New York, Chap. 5.

[5] Robertson, F. C., 1988, "Resin Transfer Molding of Aerospace Resins - A Review," Br. Polym. J., **20**, pp. 417–429.

[6] Judd, N. C. W., and Wright, W. W., 1978, "Voids and Their Effects on the Mechanical Properties of Composites—An Appraisal," SAMPE J., **14**, pp. 10–14.

[7] Olivero, K. A., Barraza, H. J., O'Rear, E. A., and Altan, M. C., 2002, "Effect of Injection Rate and Post-Fill Cure Pressure on Resin Transfer Molded Disks," J. Compos. Mater., **36**, pp. 2011–2028.

[8] Pearce, N., Guild, F., and Summerscales, J., 1998, "A Study of the Effects of Convergent Flow Fronts on the Properties of Fiber Reinforced Composites Produced by Resin Transfer Molding," Composites, Part A, **29**, pp. 141–152.

[9] Wisnom, M. R., Reynolds, T., and Gwilliam, N., 1996, "Reduction in Interlaminar Shear Strength by Discrete and Distributed Voids," Compos. Sci. Technol., **56**, pp. 93–101.

[10] Bowles, K. J., and Frimpong, S., 1992, "Void Effects on the Interlaminar Shear-Strength of Unidirectional Graphite-Fiber-Reinforced Composites," J. Compos. Mater., **26**, pp. 1487–1509.

[11] Harper, B. D., Staab, G. H., and Chen, R. S., 1987, "A Note on the Effect of Voids Upon the Hygral and Mechanical Properties of AS4/3502 Graphite/Epoxy," J. Compos. Mater., **21**, pp. 280–289.

[12] Mahale, A. D., Prud'Homme, R. K., and Rebenfeld, L., 1992, "Quantitative Measurement of Voids Formed During Liquid Impregnation of Nonwoven Multifilament Glass Networks Using an Optical Visualization Technique," Polym. Eng. Sci., **32**, pp. 319–326.

[13] Patel, N., and Lee, L. J., 1995, "Effect of Fiber Mat Architecture on Void Formation and Removal in Liquid Composite Molding," Polym. Compos., **16**(5), pp. 386–399.

[14] Patel, N., Rohatgi, V., and Lee, J. L., 1995, "Micro Scale Flow Behavior and Void Formation Mechanism During Impregnation Through a Unidirectional Stitched Fiberglass Mat," Polym. Eng. Sci., **35**, pp. 837–851.

[15] Patel, N., and Lee, J. L., 1996, "Modeling of Void Formation and Removal in Liquid Composite Molding. Part I: Wettability Analysis," Polym. Compos., **17**, pp. 96–103.

[16] Rohatgi, V., Patel, N., and Lee, J. L., 1996, "Experimental Investigation of Flow Induced Microvoids During Impregnation of Unidirectional Stitched Fiberglass Mat," Polym. Compos., **17**, pp. 161–170.

[17] Lundström, T. S., and Gebart, B. R., 1994, "Influence From Process Parameters on Void Formation in Resin Transfer Molding," Polym. Compos., **15**, pp. 25–33.

[18] Lee, C.-L., and Wei, K.-H., 2000, "Resin Transfer Molding Process (RTM) of a High Performance Epoxy Resin. II: Effects of Process Variables on the Physical, Static and Dynamic Mechanical Behavior," Polym. Eng. Sci., **40**, pp. 935–943.

[19] Darcy, H. P. G., 1856, *Les Fontaines Publiques de la Ville de Dijon*, Delmont, Paris, p. 306.

[20] Olivero, K. A., Hamidi, Y. K., Aktas, L., and Altan, M. C., 2004, "Effect of Preform Thickness and Volume Fraction on Injection Pressure and Mechanical Properties of Resin Transfer Molded Composites," J. Compos. Mater., **38**, pp. 937–958.

[21] Han, K., Lee, L. J., Nakamura, S., Shafi, A., and White, D., 1996, "Dry Spot Formation and Changes in Liquid Composite Molding: II Modeling and Simulation," J. Compos. Mater., **30**, pp. 1475–1493.

[22] Kang, M. K., Lee, W. I., and Hahn, H. T., 2000, "Formation of Microvoids During Resin-Transfer Molding Process," Compos. Sci. Technol., **60**, pp. 2427–2434.

[23] Hamidi, Y. K., Aktas, L., and Altan, M. C., 2005, "Three-Dimensional Features of Void Morphology in Resin Transfer Molded Composites," Compos. Sci. Technol., **65**, pp. 1306–1320.

[24] Hamidi, Y. K., Aktas, L., and Altan, M. C., 2004, "Formation of Microscopic Voids in Resin Transfer Molded Composites," ASME J. Eng. Mater. Technol., **126**, pp. 420–426.

[25] Barraza, H. J., Hamidi, Y. K., Aktas, L., O'Rear, E. A., and Altan, M. C., 2004, "Porosity Reduction in the High-Speed Processing of Glass Fiber Composites by Resin Transfer Molding (RTM)," J. Compos. Mater., **38**, pp. 195–226.

[26] Hamidi, Y. K., and Altan, M. C., 2003, "Spatial Variation of Void Morphology in Resin Transfer Molded E-Glass/Epoxy Composites," J. Mater. Sci. Lett., **22**, pp. 1813–1816.

[27] Breard, J., Saouab, A., and Bouquet, G., 2003, "Numerical Simulation of Void Formation in LCM," Composites, Part A, **34**, pp. 517–523.

[28] Binetruy, C., Hilaire, B., and Pabiot, J., 1998, "Tow Impregnation Model and Void Formation Mechanisms During RTM," J. Compos. Mater., **32**, pp. 223–245.

[29] Chang, C.-Y., and Hourng, L.-W., 1998, "Study on Void Formation in Resin Transfer Molding," Polym. Eng. Sci., **38**, pp. 809–818.

[30] Thomas, M. M., Joseph, B., and Kardos, J. L., 1997, "Experimental Characterization of Autoclave-Cured Glass-Epoxy Composite Laminates: Cure Cycle Effects Upon Thickness, Void Content and Related Phenomena," Polym. Compos., **18**, pp. 283–299.

[31] Chan, A. W., and Morgan, R. J., 1992, "Modeling Preform Impregnation and Void Formation in Resin Transfer Molding of Unidirectional Composites," Polym. Compos., **23**, pp. 48–52.

[32] Lundstrom, T. S., Gebart, B. R., and Lundemo, C. Y., 1993, "Void Formation in RTM," J. Reinf. Plast. Compos., **12**, pp. 1339–1349.

[33] Rajulu, A. V., Chary, K. N., Reddy, G. R., and Meng, Y. Z., 2004, "Void Content, Density and Weight Reduction Studies on Short Bamboo Fiber-Epoxy Composites," J. Reinf. Plast. Compos., **23**, pp. 127–30.

[34] Stabler, W. R., Tatterson, G. B., Sadler, R. L., and El-Shiekh, A. H. M., 1992, "Void Minimization in the Manufacture of Carbon Fiber Composites by Resin Transfer Molding," Science and Engineering of Composite Materials, **23**, pp. 38–42.

[35] Ghiorse, S. R., 1991, "A Comparison of Void Measurement Methods for Carbon/Epoxy Composites," U.S. Army Materials Technology Laboratory, Report No. MTL TR 91-13.

[36] Santulli, C., Garcia Gil, R., Long, A. C., and Clifford, M. J., 2002, "Void Content Measurements in Thermoplastic Composite Materials Through Image Analysis From Optical Micrographs," Science and Engineering of Composite Materials, **10**, pp. 77–90.

[37] Shih, C.-H., 2000, "Liquid Composite Molding of Tackified Fiber Reinforce-

ment: Preforming and Void Removal," Ph.D. thesis, Ohio State University, Columbus, OH.
[38] Shi, D., and Winslow, D., 1990, "Accuracy of a Volume Fraction Measurement Using Areal Image Analysis," J. Test. Eval., **19**(3), pp. 210–213.
[39] Merle, G., Allemand, J., Camino, G., Luda, M. P., Revellino, M., and Blancon, R., 1998, "Morphology Analysis of Microvoids in SMC: Aging Effects," Composites, Part A, **29**, pp. 1535–1543.
[40] Howe, C. A., Paton, R. J., and Goodwin, A. A., 1997, "A Comparison Between Voids in RTM and Prepreg Carbon/Epoxy Laminates," *Proceedings of ICCM-11*, M. L. Scott, ed., Australian Composite Structures Society, Vol. IV, pp. 46–51.
[41] Goodwin, A. A., Howe, C. A., and Paton, R. J., 1997, "The Role of Voids in Reducing the Interlaminar Shear Strength in RTM Laminates," *Proceedings of ICCM-11*, M. L. Scott, ed., Australian Composite Structures Society, Vol. IV, pp. 11–19.